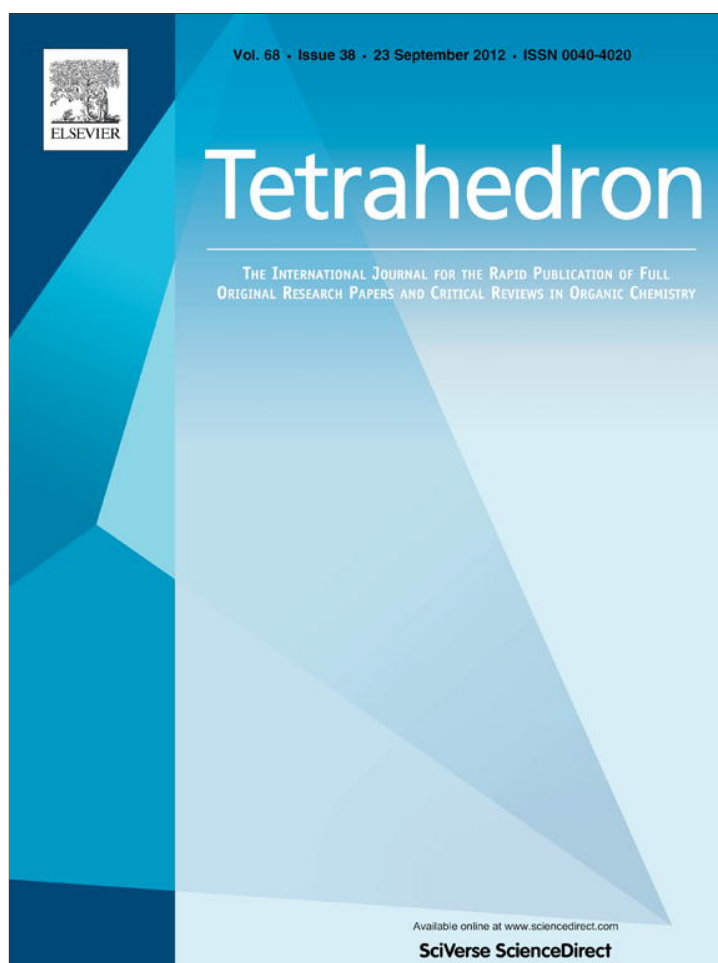


Provided for non-commercial research and education use.
Not for reproduction, distribution or commercial use.



This article appeared in a journal published by Elsevier. The attached copy is furnished to the author for internal non-commercial research and education use, including for instruction at the authors institution and sharing with colleagues.

Other uses, including reproduction and distribution, or selling or licensing copies, or posting to personal, institutional or third party websites are prohibited.

In most cases authors are permitted to post their version of the article (e.g. in Word or Tex form) to their personal website or institutional repository. Authors requiring further information regarding Elsevier's archiving and manuscript policies are encouraged to visit:

<http://www.elsevier.com/copyright>



Contents lists available at SciVerse ScienceDirect

Tetrahedron

journal homepage: www.elsevier.com/locate/tet

Synthesis, metal ion binding, and photochromic properties of benzo- and naphthopyrans annelated by crown ether moieties

Sergey V. Paramonov^{a,*}, Vladimir Lokshin^b, Artem B. Smolentsev^c, Evgeni M. Glebov^c, Valeri V. Korolev^c, Stepan S. Basok^d, Konstantin A. Lysenko^{a,†}, Stéphanie Delbaere^e, Olga A. Fedorova^{a,†}

^aA.N. Nesmeyanov Institute of Organoelement Compounds, Russian Academy of Sciences, 28 Vavilova St., 119991 Moscow, Russian Federation

^bCentre Interdisciplinaire de Nanoscience de Marseille (CINaM, CNRS UMR 7325), Aix-Marseille Université, 163 Av. de Luminy, 13288 Marseille, France

^cInstitute of Chemical Kinetics and Combustion, Siberian Branch of Russian Academy of Sciences, 3 Institutskaya St., 630090 Novosibirsk, Russian Federation

^dA.V. Bogatsky Physico-Chemical Institute, National Academy of Science of Ukraine, 86 Lustdorfskaya doroga, 650080 Odessa, Ukraine

^eUniversité Lille Nord de France, CNRS UMR 8516, UDSL 3 rue du Professeur Laguesse BP83, 59006 Lille, France

ARTICLE INFO

Article history:

Received 28 February 2012

Received in revised form 17 June 2012

Accepted 10 July 2012

Available online 20 July 2012

Keywords:

Chromenes

Crown ether

Synthesis

Baeyer–Villiger oxidation

Host–guest complexes

Binding constants determination

Photochromism

ABSTRACT

Combining a photochromic chromene with a crown ether moiety results in systems in which photochromism and ionophoric properties could significantly influence each other. In this paper, we report the synthesis of several chromenes annelated by 15(18)-crown-5(6) ethers. The approach involves the building of the photochromic fragment upon the initial crown ether via phenols. The two main routes for chromene preparation are discussed. The complex formation of the synthesized photochromic crown-containing naphthopyran with magnesium(II) and barium(II) cations was studied. The kinetic behavior of the colored form of the compound is affected by complex formation.

© 2012 Elsevier Ltd. All rights reserved.

1. Introduction

Photochromic systems have the ability to undergo a reversible transformation between two states giving rise to different absorption spectra, induced, at least in one direction, by electromagnetic radiation.¹ If one of the states absorbs in the visible region under appropriate conditions, a noticeable, reversible change of color occurs as a consequence of the transformation. Photo-transformations of this type open a wide field of potential applications in modern technologies, such as optical switches, memories, and molecular electronics.² In recent research, the photochemically-reversible construction of nanoarchitectures,³ the introduction of photochromic molecules into supramolecular

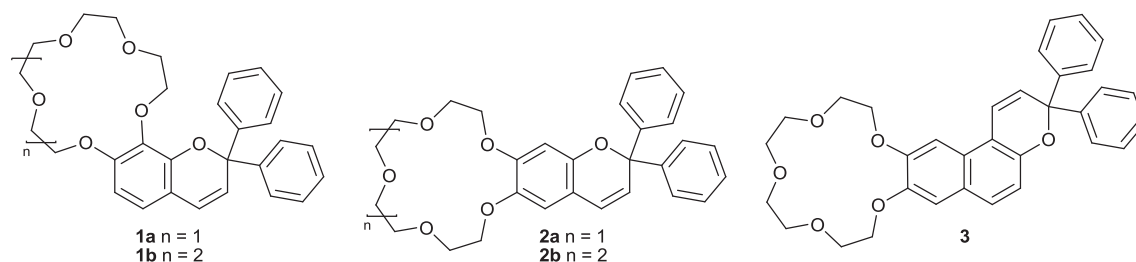
assemblies,⁴ and biological photoswitching systems⁵ have also been realized.

Attaching a crown ether moiety to a photochromic molecule leads to substantial extension of the possible practical usage of such systems.⁶ Different chromenes linked to a macrocyclic fragment have already been reported.⁷ However, there is a lack of information concerning the synthesis of photochromes annelated by a crown ether moiety. Meanwhile, we believe that annelation of the ionophoric moiety should lead to a more considerable mutual influence of the two processes that occur in the molecule, namely complex formation and the photoinduced transformation.

Recently, we reported for the first time the synthesis of angular chromenes annelated by 15(18)-crown-5(6) ethers **1a,b**.⁸ In the present paper, we extend the series and describe new linear chromenes **2** and naphthopyran **3**. The presented synthesis involves general routes to photochromic systems annelated by a crown ether fragment. For naphthopyran **3**, we have also studied photochromic properties and complex formation with magnesium(II) and barium(II) cations.

* Corresponding author. Tel.: +7 499 135 80 98; fax: +7 499 135 50 85; e-mail addresses: paramonov@ineos.ac.ru (S.V. Paramonov), fedorova@ineos.ac.ru (O.A. Fedorova).

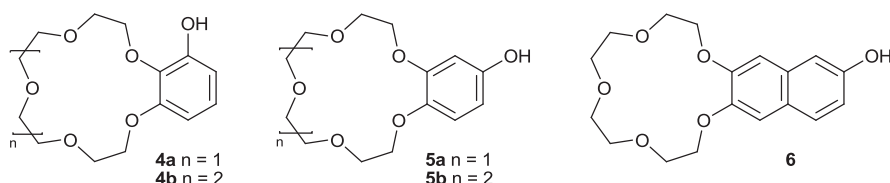
† Tel.: +7 499 135 80 98; fax: +7 499 135 50 85.



2. Results and discussion

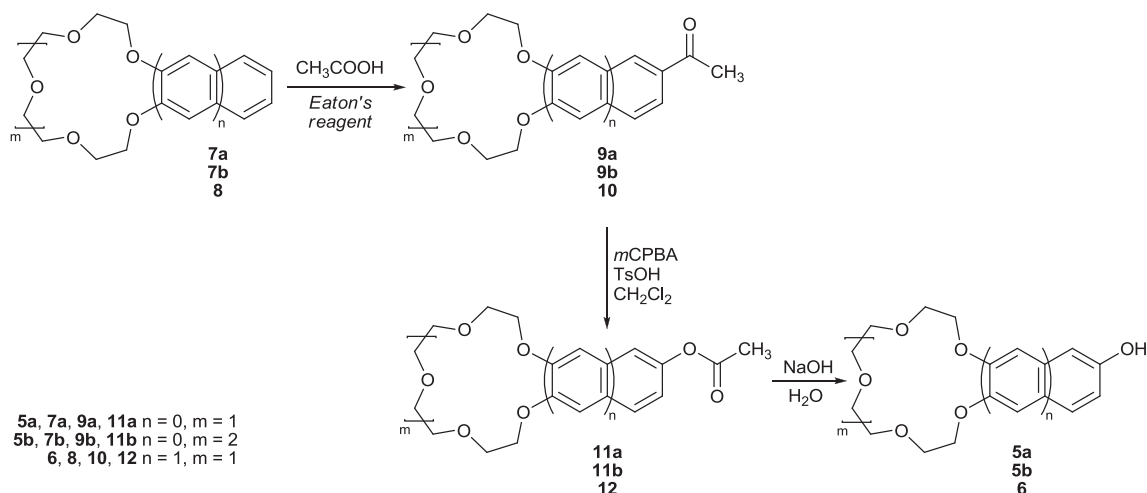
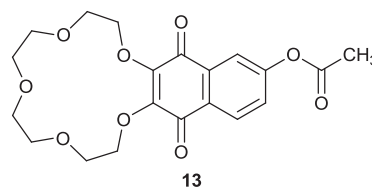
2.1. Synthesis

Phenols or naphthols are known to be suitable precursors for chromene synthesis.¹ However, only a small number of crowned phenols are commercially available. In most cases, the corresponding benzo- or naphthocrown ether is transformed into the hydroxy-substituted derivative. In addition, certain substitution requires the application of specific synthetic approaches involving crown ether constructing upon the phenol system, e.g., phenols **4**.⁸



In the synthesis of compounds **2** and **3**, the starting phenols **5** and naphthol **6** were synthesized from the available benzo-15(18)-crown-5(6) and naphtho-15-crown-5 ethers. A modification of the approach firstly reported by Wada et al.⁹ was used. The synthesis was based on a selective acylation of benzene (**7**) or naphthalene (**8**) derivative, followed by the restoration of ketones **9** and **10** into ester functions, and further base hydrolysis of esters **11**, **12** to give crown-containing phenols **5** or naphthol **6** (Scheme 1).

latter from the reaction mixture by column chromatography. Among the side-products of ketone **10** oxidation, quinoid derivative **13** was identified (consult Supplementary data for details).



Scheme 1. The preparation of crown-containing phenols **5** and **6**.

Further treatment of esters **11** and **12** with 10% aqueous NaOH resulted in phenols **5b** (50%) and **6** (60%) [93% and 82% for **5a** and **5b**, respectively, in lit.⁹]. The X-ray structure of new naphthol **6** is presented in Fig. 1. Compound **6** crystallizes as a solvate with water

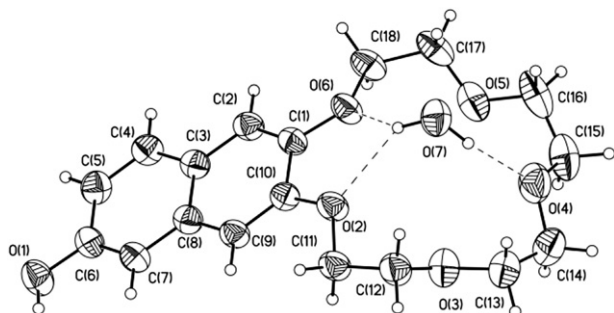


Fig. 1. The general view of **6** in representation of atoms by thermal ellipsoids ($p=50\%$).

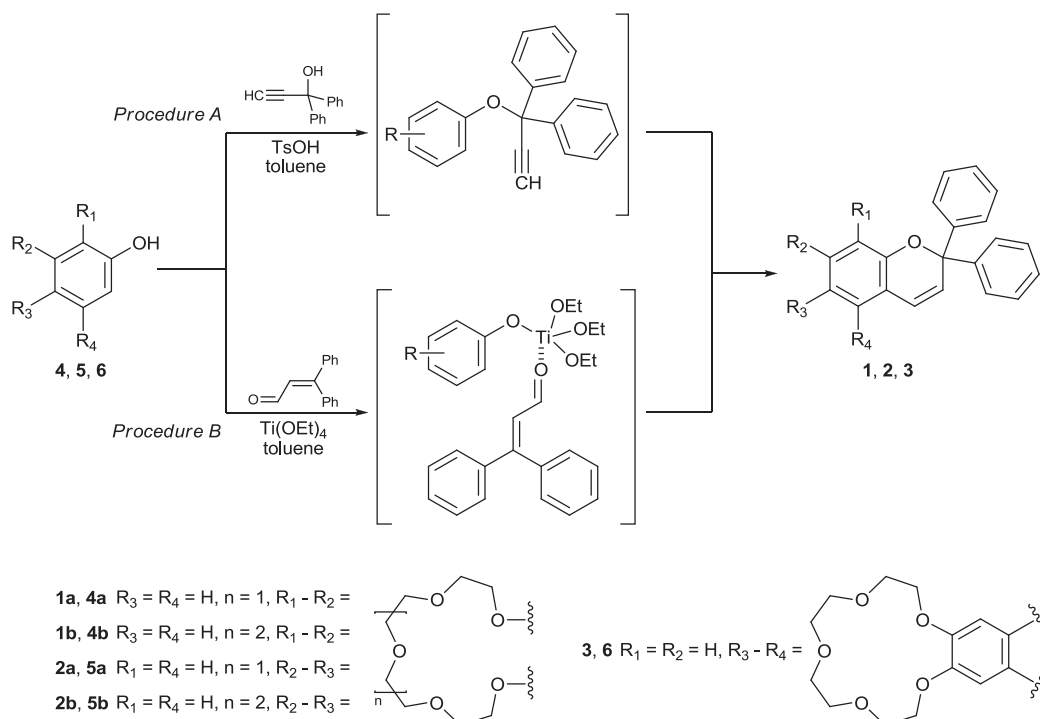
and CH_2Cl_2 molecules. The bond lengths and angles in **6** are close to those expected. The water molecule serves both as a proton donor and acceptor participating in H-bonds with oxygen atoms of the crown ether ($\text{O}\cdots\text{O}$ 2.817–3.052(7) Å) and with the hydroxyl group ($\text{O}\cdots\text{O}$ 2.730(6) Å) resulting in the formation of the infinite helix consisting of alternating **6** and water molecules and directed along crystallographic axis b . The CH_2Cl_2 molecule disordered over three positions is situated within the folds of the above-mentioned helix and is likely to participate in a number of weak $\text{C}\cdots\text{H}\cdots\text{O}$ and $\text{C}\cdots\text{H}\cdots\text{Cl}$ contacts.

2*H*-Chromene derivative preparation procedures are based on a 'one-pot reaction' starting from a suitable phenol or naphthol. In our research, two different methods were used. *Procedure A* involves the acid-catalyzed reaction of phenols or naphthols with propargylic alcohol.¹¹ The reaction proceeds via Claisen rearrangement of alkylnyl aryl ethers resulting from naphthol 'O-alkylation', followed by [1,5]*H* sigmatropic shift and electrocyclic

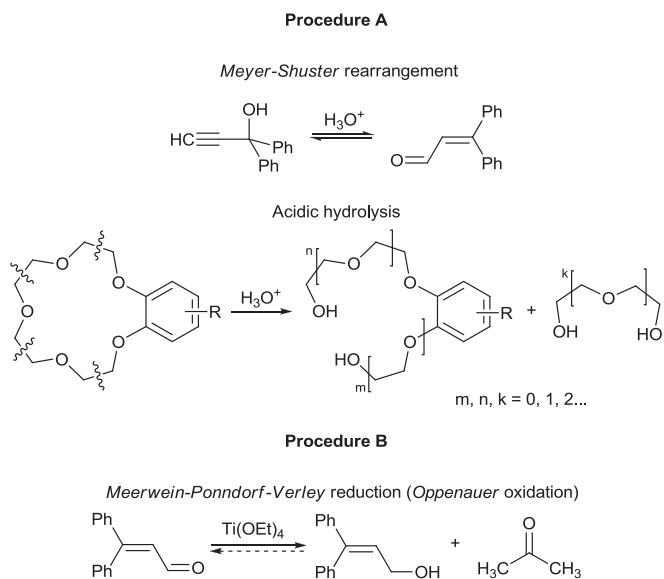
ring closure. Another approach (*Procedure B*) suggests condensation of phenols or naphthols with β -phenylcinnamaldehyde in the presence of titanium(IV) ethoxide (Scheme 2).¹²

Procedure A was originally applied for preparation of carbocyclic chromenes and *Procedure B* was developed for heterocyclic chromene synthesis. The latter may be successfully used for carbocyclic chromenes, too. However, in the case of crown containing chromenes, *Procedure B* has significant advantages despite the early reports of its lack of success.¹³ The main disadvantages of *Procedure A* are the side-processes involving PTSA interactions with reagents that diminish yields and make the purification of the product difficult. In the presence of PTSA the diphenylpropargylic alcohol transforms into β -phenylcinnamaldehyde via a Meyer–Shuster rearrangement mechanism (Scheme 3, procedure A), the aldehyde being isolated in this study in negligible amount. Apparently, the acidic conditions also lead to partial hydrolysis of the crown ether resulting in impurities containing different polyether substitution that significantly hinder the product isolation (Scheme 2, procedure A). On the contrary, *Procedure B* does not have these disadvantages. It allows higher yields generally due to easier separation of the reaction mixture. However, a few products of side reactions involving the aldehyde and titanium(IV) ethoxide interaction probably via a Meerwein–Ponndorf–Verley reduction mechanism are suggested (Scheme 3, procedure B), and 3,3-diphenylprop-2-en-ol has been separated out. Nevertheless these reactions do not affect considerably the main product isolation.

The yields for chromene preparation are summarized in Table 1 and they are usual for chromene synthesis. The structures of the products were confirmed by NMR spectroscopy and elemental analysis. The X-ray investigation was performed for compound **1a** (Fig. 2). The conformation of the oxygen containing cycle can be described as a distorted sofa with the deviation of O(1) and C(10) atoms from the mean plane of the other atoms by 0.65 and 0.30 Å. According to the bond length distribution in the aromatic cycle as well as values of lengths for C(6)–C(7) and C(5)–C(6) bonds (1.325(2) Å and 1.447(2) Å, respectively) one may conclude that the



Scheme 2. The principal routes to chromenes.



Scheme 3. Main side reactions of the methods.

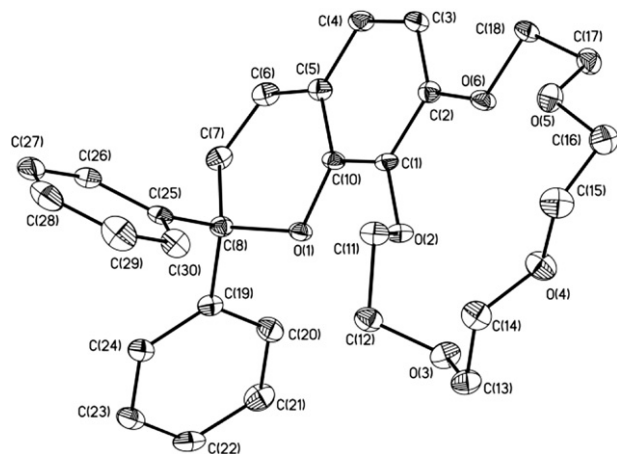
Table 1
The chromenes preparation yields

	1a $n=1$	1b $n=2$	2a $n=1$	2b $n=2$	3
Procedure A	<1%	<1%	4%	19%	16%
Procedure B	30%	30%	20%	25%	29%

C(6)–C(7) double bond practically does not participate in conjugation with the aromatic system. The analysis of intermolecular contacts revealed that all of them correspond to weak van-der-Waals type contacts.

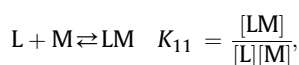
2.2. Complex formation

The crown ether fragment in the molecule of naphthopyran **3** gives it the ability to form stable complexes with alkaline-earth

Fig. 2. The general view of **1a** in representation of atoms by thermal ellipsoids ($p=50\%$).

metal cations.¹⁴ In our study, we chose Mg^{2+} and Ba^{2+} , which have different ionic radii. The stoichiometry and stability constants of the complexes were determined by two common optical methods, namely Job's plot and spectrophotometric titration.¹⁵

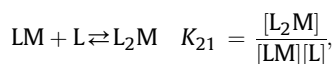
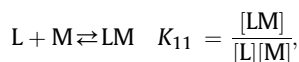
Fig. 3a demonstrates the formation of the complex between naphthopyran **3** and Mg^{2+} . The isosbestic points (307 and 360 nm, Fig. 3a) supports the assumption that only two forms containing the chromene molecule coexist in solution. The Job's plot method was used to determine the stoichiometry of the complexes.^{15a} According to the Job's plot the ratio of naphthopyran **3** to Mg^{2+} in the complex is 1:1 (Fig. 3b). Taking into account the radius of the 15-crown-5-ether cavity (0.85 Å)¹⁴ and the ionic radius of Mg^{2+} (0.72 Å),¹⁴ we suggest the formation of an inclusive 1:1 complex, in which the cation is located inside the crown ether. The stability constant of the complex was determined from the observed absorbance changes in the course of the titration (Fig. 3c, Table 2) considering the following equilibrium:



where K_{11} corresponds to the stability constant of the 1:1 complex; [L], [M], and [LM] denote the equilibrium concentration of the

metal cations, naphthopyran (ligand), and their 1:1 complex, respectively. The data was analyzed by numerical methods described elsewhere¹⁶ (consult Supplementary data for details).

In the case of barium cations, the UV–vis spectra during titration showed no isosbestic points indicating the existence of more than one complex in the solution (Fig. 4a). Analysis of the experimental data (Fig. 4b) revealed the presence of two types of complex, namely with ligand to metal (L/M) composition equal to 1:1 and 2:1. The stability constants were determined considering the following equilibria (Fig. 4b, Table 2):



where K_{11} and K_{21} correspond to the stability constants of the 1:1 and 2:1 complexes; [L], [M], [LM], [L₂M] denote the equilibrium concentration of the metal cations, naphthopyran (ligand), and their 1:1 and 2:1 complexes, respectively. The ionic radius of Ba^{2+} is 1.36 Å,¹⁴ which is larger than the crown ether cavity radius. Therefore, we suggest the formation of an exclusive 1:1 complex, in which the cation is located outside the crown ether fragment, and a sandwich 2:1 complex (Scheme 4), which is stabilized by the stacking interaction of the two chromene molecules.^{17,18}

The magnesium 1:1 complexes are generally more stable than the corresponding barium complexes due to the higher charge density of the cation and its size that fits well the crown ether

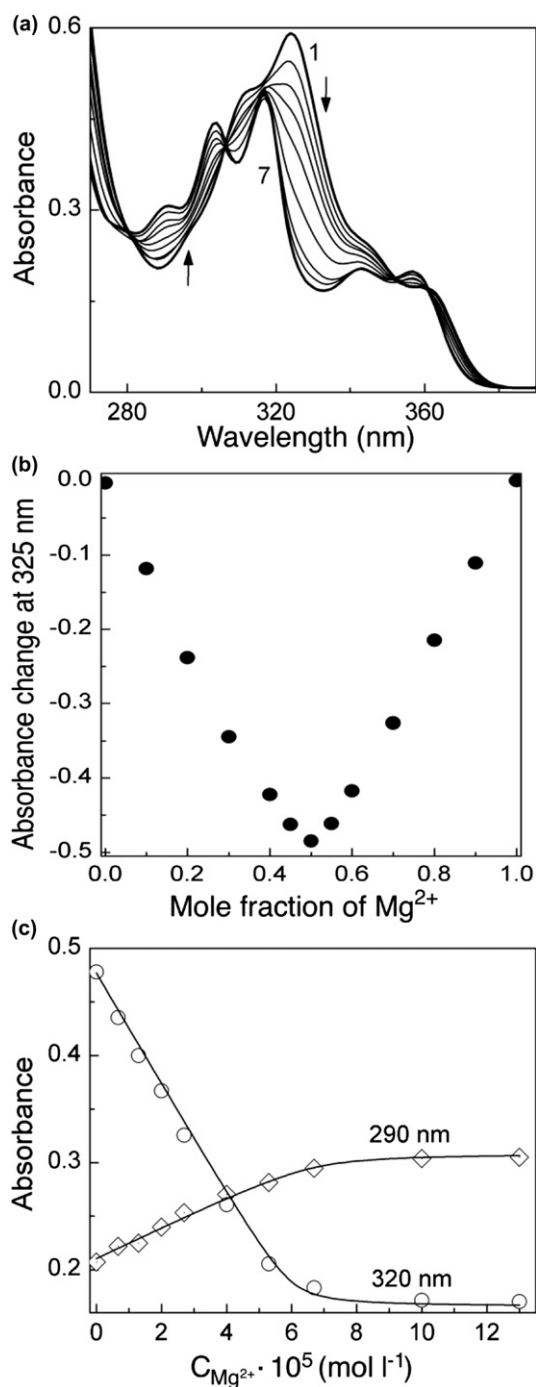


Fig. 3. Complex formation of naphthopyran **3** with magnesium(II) cations in acetonitrile: (a) spectrophotometric titration of **3** with solution of $\text{Mg}(\text{ClO}_4)_2$, cuvette 1 cm, $C_3=6 \times 10^{-5}$ M, curves 1–9 correspond to 0, 6×10^{-6} , 1.2×10^{-5} , 1.8×10^{-5} , 2.4×10^{-5} , 3×10^{-5} , 4.8×10^{-5} , 6×10^{-5} , and 1.2×10^{-4} M of $\text{Mg}(\text{ClO}_4)_2$, respectively; (b) Job's plot for complex formation between **3** and Mg^{2+} , the sum of **3** and Mg^{2+} concentrations being constant and equal to 1.2×10^{-4} M; (c) determination of the stability constant: dots represent experimental data, solid lines correspond to calculated dependencies of absorbance on metal cations concentration (consult [Supplementary data](#) for details).

Table 2
Stability constants of the complexes of naphthopyran **3** with metal cations in CH_3CN

Cation	$\log K_{11}$	$\log K_{21}$
Mg^{2+}	6.0 ± 0.3	—
Ba^{2+}	4.2 ± 0.4	4.9 ± 0.3

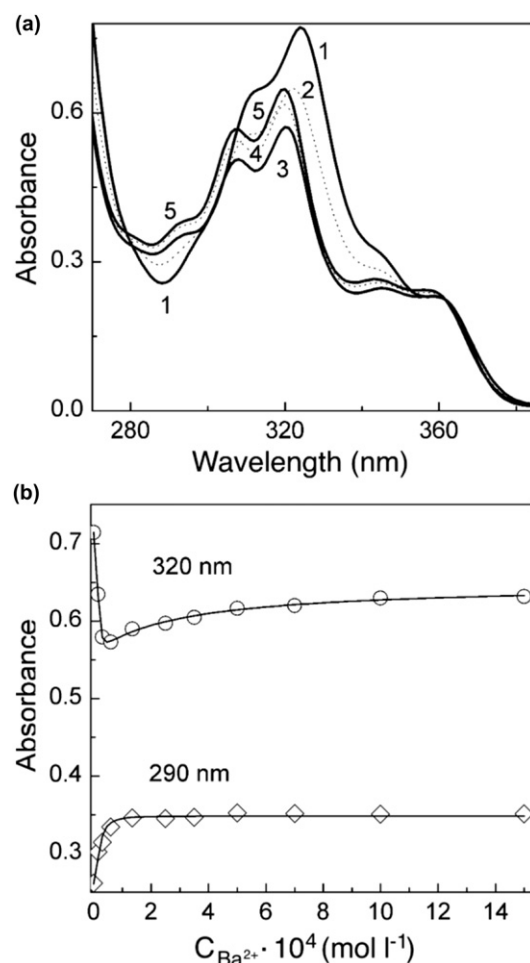


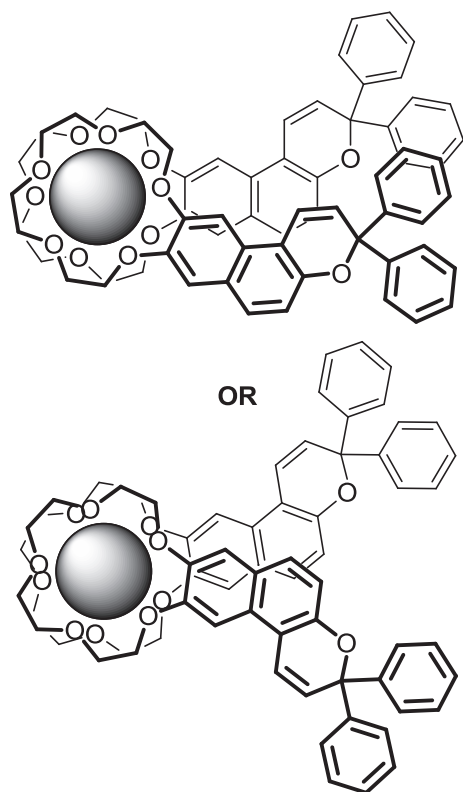
Fig. 4. Complex formation of naphthopyran **3** with barium(II) cations in acetonitrile: (a) spectrophotometric titration of **3** with solution of $\text{Ba}(\text{ClO}_4)_2$, cuvette 1 cm, $C_3=9 \times 10^{-5}$ M, curves 1–5 correspond to 0, 1.5×10^{-5} , 9×10^{-5} , 5×10^{-4} , and 1.5×10^{-3} M of $\text{Ba}(\text{ClO}_4)_2$; (b) determination of stability constant: dots represent experimental data, solid lines correspond to calculated dependencies of absorbance on metal cation concentration (consult [Supplementary data](#) for details).

cavity.¹⁴ This finding as well as the formation of the sandwich complexes with Ba^{2+} are consistent with our previous results with other ligands.¹⁹

To support the UV–vis studies, we performed a series of NMR investigations of ligand **3** and its complexes with Mg^{2+} and Ba^{2+} . Addition of the cations led to significant changes of the spectra evidencing complex formation. Thus, in the presence of magnesium cations, all the signals were shifted downfield as a result of the electron-withdrawing effect of the cation bound by the crown ether (Fig. 5).

In the case of barium cations, the spectral changes were more complex. At ambient temperature, the addition of the cation to a solution of the ligand led to a significant broadening of the NMR signals caused by fast chemical exchange of the corresponding nuclei and cation-induced paramagnetic relaxation.²⁰ Lowering the temperature to -40 °C allowed us to enhance the resolution and perform the analysis. Two solutions with different ligand-to-cation ratios were studied assuming the complexation scheme determined from the UV–vis experiments (Fig. 6).

The NMR spectrum of a solution with excess of Ba^{2+} (1:9 ratio) reflected one dominating component, which was attributed to the 1:1 complex. All the signals were shifted downfield in the same way we observed with magnesium cations. The spectra of the solution with 2:1 ratio were more complex and contained two distinguishable families of peaks. Performing a series of 2D NMR



Scheme 4. Possible structures of the sandwich complexes of **3** with Ba^{2+} cations with symmetric (up) and asymmetric (bottom) arrangement of the ligand molecules.

experiments allowed us to assign the signals (see [Supplementary data](#)). Similarly to the 1:1 complex, the aliphatic protons were shifted downfield evidencing for the cation located in the crown ether cavity. However, most of the aromatic protons were strongly shifted upfield. Noteworthy, the shifts were essentially the same for the both components in the spectra.

Taking into account the two possible complex structures, we propose the following analysis of the observed data. The structure of the symmetric complex suggests that all aromatic protons should experience shielding effect from the aromatic system of the

opposite molecule. On the other hand, in the asymmetric complex, such an effect should be experienced by only H-5, 6, 7, and 10, while H-1 and H-2 should have different effects. The observed changes (for the both components) in chemical shifts correlate better with the asymmetric model. Protons H-6, 7, and 10 are strongly shielded, proton H-5 is less affected (probably, due to mutually exclusive deshielding and shielding effects). Protons H-1 and H-2 should experience deshielding effect from the cation. Indeed, H-1 is shifted downfield. The observed position of proton H-2 is possibly due to specific position of the phenyl groups, which may have changed their position in the sandwich complex so that one of the phenyls is located close to H-2. According to this hypothesis, the two components in the spectra correspond to different conformations of the complex with more or less extent of rotation of the ligands relatively each other.

2.3. Photochromic properties

Generally, upon irradiation with UV light, naphthopyran **3** should convert into so-called open forms (TC and TT), which absorb in visible region ([Scheme 5](#)).²¹ Upon cessation of irradiation, the colored forms transform back into the initial closed form, the process being biexponential in general. Irradiation of the solution of **3** in acetonitrile with 313 nm (filtered light) leads to evolution of the broad adsorption band with $\lambda_{\text{max}}=425$ and a shoulder at ca. 500 nm ([Fig. 7a](#)). In our case at ambient temperature, the bleaching was characterized by a monoexponential curve ([Fig. 7b](#)), the observed bleaching rate constant being $0.15 \pm 0.02 \text{ s}^{-1}$, which corresponds to half-life time of ca. 5 s. The monoexponential dependence could virtually indicate the formation of only one open isomer (presumably, TC) and is most probably due to relatively short irradiation time (20 s) insufficient to reach the photostationary state. Indeed, parallel NMR investigations at -40°C , when the bleaching is significantly retarded and hence the TC concentration becomes sufficient to trigger the TT formation, revealed the formation of the TT form only after 30 min of irradiation ([Fig. 8](#)).

The addition of metal cations to the solutions did not change the position of the absorption maximum of the open form, yet it altered the persistence of the colored forms. The bleaching rate constant was increasing along with the increasing concentrations of the metal ([Fig. 9](#)). However, after a certain concentration, the

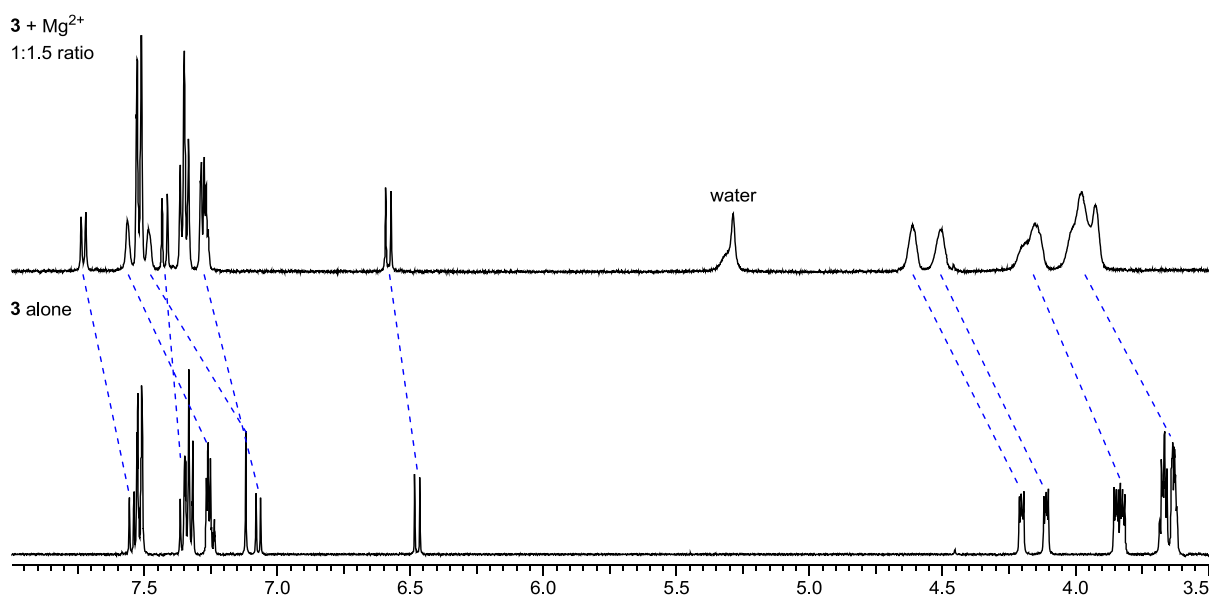


Fig. 5. ^1H NMR spectra of **3** and its mixture with Mg^{2+} ($C_3/C_{\text{Mg}}=1:1.5$) at 20°C (CD_3CN , $C_3=0.001 \text{ M}$).

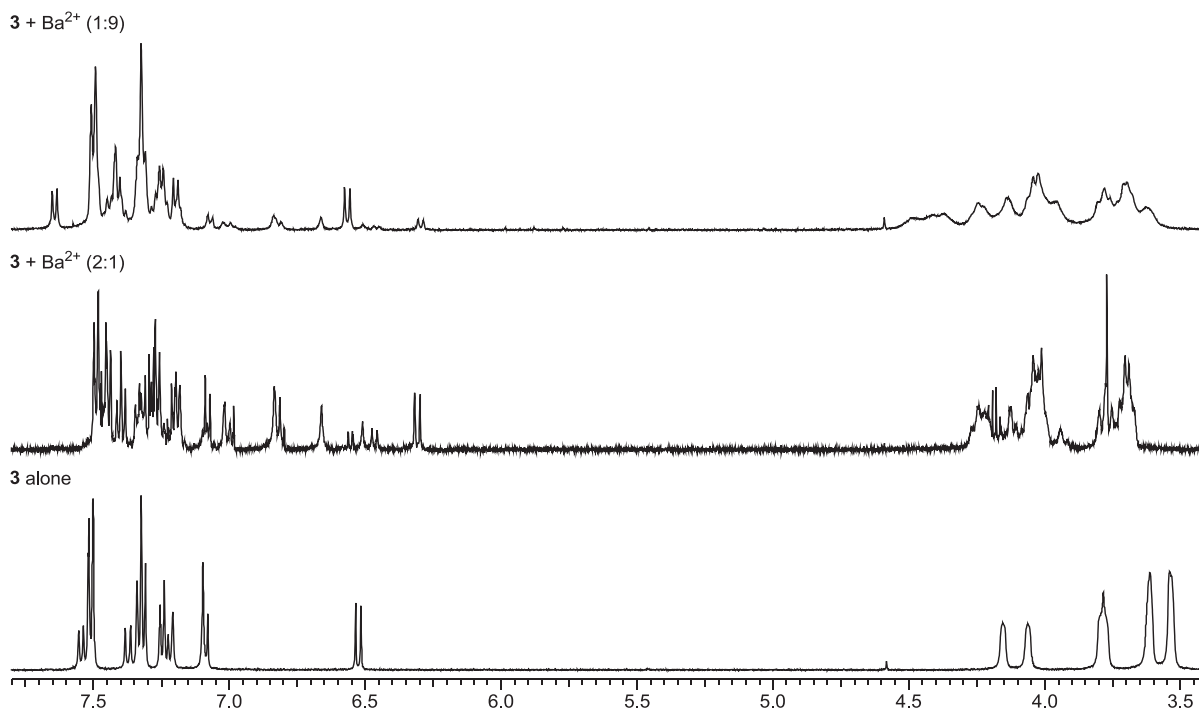
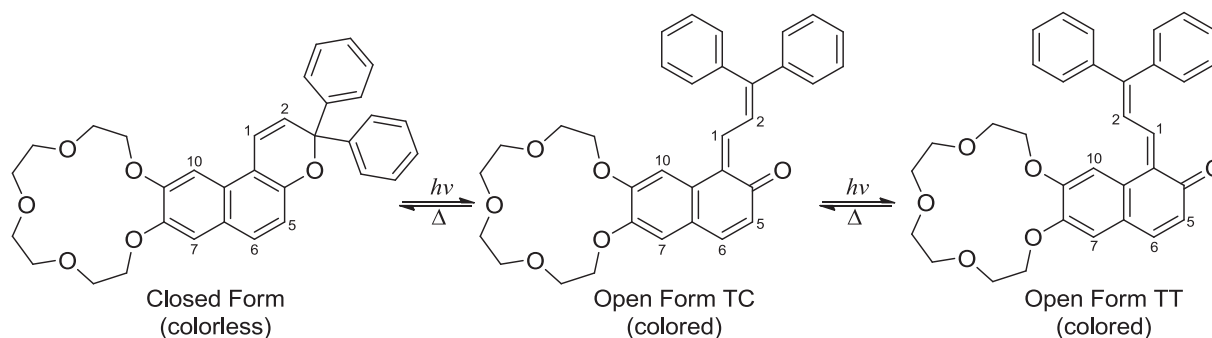


Fig. 6. ^1H NMR spectra of **3** and its mixtures with Ba^{2+} ($C_3/C_{\text{Ba}}=2:1$ and $1:9$) at -40°C (CD_3CN , $C_3=0.0056\text{ M}$ and 0.001 M , respectively).



Scheme 5. The photochromic transformation of naphthopyran **3**.

dependencies evolved into plateaus, the limiting values being 0.55 and 0.37 s^{-1} for Mg^{2+} and Ba^{2+} , respectively. Thus, complex formation with metal cations leads to partial destabilization of the open form of the naphthopyran. These results are consistent with our previous findings for chromene **2a**.¹⁸

Unfortunately, instability of the open forms in the presence of cations even at low temperature hindered the NMR investigations. Still the observed characteristic peaks of the TC form were shifted downfield evidencing for the transformation of the complexed CF forms into the TC isomers (Fig. 10).

3. Conclusions

Here, we described the multistep synthesis of new naphtho- and benzopyrans annelated by crown ether fragments. The main precursors are crown-containing phenols and naphthols. They could be considered as promising for preparation of wide choice of derivatives. Improved conditions of the Baeyer–Villiger rearrangement were found for their preparation. Another important achievement of the synthetic approach is employing phenol or naphthol condensation with β -phenylcinnamaldehyde in the presence of titanium(IV) ethoxide (*Procedure B*). This method is not

well developed in comparison with the one which involves the acid-catalyzed reaction of phenols with propargylic alcohol (*Procedure A*). However, in the case of these crown containing chromenes, *Procedure B* appeared to be more appropriate, the yields being not high but rather good for chromene synthesis.

The complex formation and the photochromic behavior of naphthopyran **3** were also demonstrated. The compound forms the $1:1$ complexes with both magnesium(II) and barium(II) cations and also the $2:1$ sandwich complexes with barium(II) cations. The presence of metal cations in the solution leads to partial destabilization of the photoinduced form of **3** and consequently decreases its lifetime. Nevertheless, complexation does not shift the maxima of absorption of the merocyanine form. This phenomenon may be employed for creation of new photochromic sensors on metal ions.

4. Experimental section

4.1. Experimental procedures and characterization data

Column chromatography was performed using chromatography silica ($40\text{--}63\ \mu\text{m}$ particle size distribution). Melting points

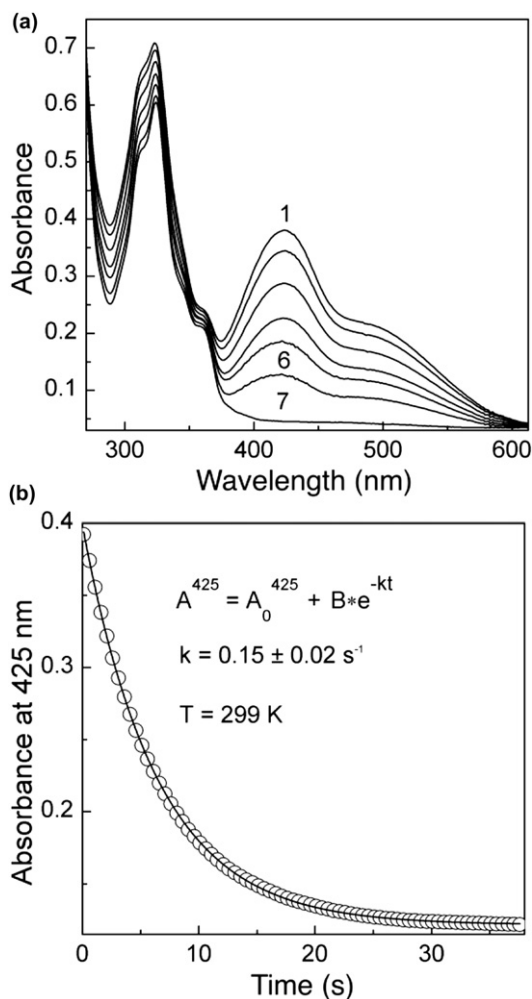


Fig. 7. Thermal bleaching of naphthopyran **3** in acetonitrile solution ($C_3=1.2 \times 10^{-4} \text{ M}$, cuvette 1 cm): (a) changes in the UV spectra, curve 1 corresponds to a spectrum after 20 s irradiation at 313 nm, curves 2–6 correspond to 1, 3, 5, 8, and 15 s after cessation of irradiation, curve 7 corresponds to the chromene's spectrum prior to irradiation; (b) kinetic curve of the thermal relaxation monitored at 425 nm.

were determined in capillary tubes and are uncorrected. NMR spectra were recorded on a Bruker Avance 250 MHz instrument for solutions in CDCl_3 unless otherwise stated; δ values are given in parts per million, coupling constants are quoted in hertz. Melting points were not corrected. All chemicals were purchased from Aldrich, Acros or AlfaAesar and used without additional purification.

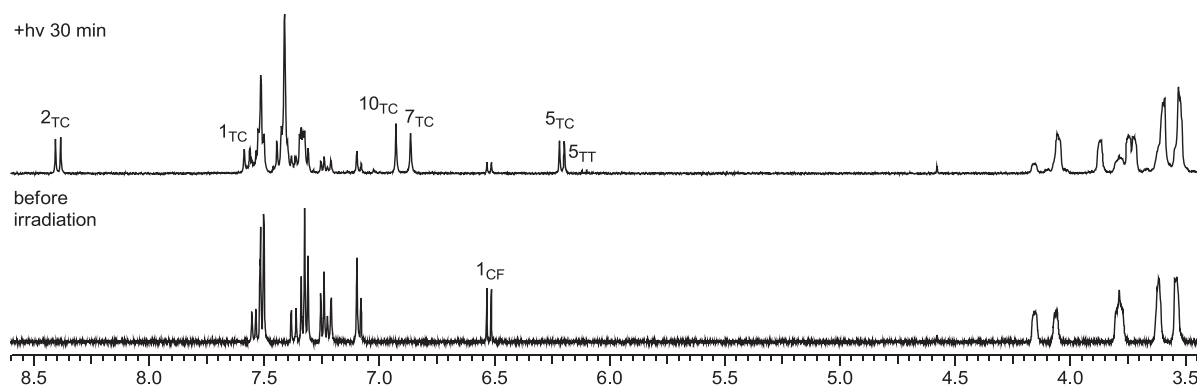


Fig. 8. ^1H NMR spectra of **3** irradiated at 313 nm (-40°C , CD_3CN , $C_3=0.001 \text{ M}$).

Angular chromenes containing 15(18)-crown-5(6) ether moieties **1** and the synthesis of the corresponding crowned phenols **4** were earlier reported.⁸ Compounds **5a,b**, **9a,b**, **11a,b** were first described by Wada et al.⁹ Benzo-crown ethers **7** are commercially available. Naphtho-15-crown-5 ether **8** was synthesized according to lit.²²

4.2. 1-(2,3,5,6,8,9,11,12-Octahydronaphtho[2,3-b][1,4,7,10,13]pentaoxacyclopentadecine-16-yl)ethanone (**10**)

A modification of the previously reported procedure²³ was used. Commercially available Eaton's reagent (ca. 8 ml that corresponds to 6.28 mmol of phosphorus(V) oxide) and acetic acid (0.20 ml, 3.45 mmol) were mixed at room temperature. Then naphtho-15-crown-5 ether (1 g, 3.14 mmol) was added. The reaction mixture was stirred at room temperature for ca. 6 h and then poured into water. The suspension was extracted with dichloromethane and the combined organic phases were washed with water. Removal of the dried (MgSO_4) solvent gave a dark brown oil, which upon repeated extractions with hot heptane, afforded the product as an off-white solid (1.02 g, 90%), mp $126\text{--}129^\circ\text{C}$. ^1H NMR (250 MHz, CDCl_3): δ 2.69 (s, 3H, CH_3), 3.78–3.76 (m, 8H, 5'- CH_2 , 6'- CH_2 , 8'- CH_2 , 9'- CH_2), 3.96–4.06 (m, 4H, 3'- CH_2 , 11'- CH_2), 4.22–4.32 (m, 4H, 2'- CH_2 , 12'- CH_2), 7.11 (s, 1H, 19'-H), 7.20 (s, 1H, 14'-H), 7.70 (d, $J=8.6 \text{ Hz}$, 1H, 18'-H), 7.89 (dd, $J=8.6$ and 1.5 Hz , 1H, 17'-H), 8.31 (s, 1H, 15'-H). ^{13}C NMR (250 MHz, CDCl_3): δ 26.67, 68.50, 68.60, 69.32, 69.39, 70.37, 70.40, 71.41, 107.40, 109.15, 122.79, 126.72, 128.41, 128.60, 132.27, 133.14, 149.95, 151.48, 198.16. Anal. Calcd for $\text{C}_{20}\text{H}_{24}\text{O}_6$: C, 66.65; H, 6.71. Found: C, 66.37; H, 6.68.

4.3. Typical procedure for Bayer–Villiger oxidation

An adaptation of the previously reported procedures^{9,10a} was used. *m*-Chloroperbenzoic acid (70%, 3 mmol) was added to a stirred solution of ketone **10** (1.5 mmol), TsOH (1 mmol) in dichloromethane (10 ml) in a single portion. The mixture was stirred at room temperature overnight under argon atmosphere, then filtered and the precipitate formed was washed with dichloromethane. The organic phase was washed with 10% aqueous sodium bisulfite solution ($2 \times 20 \text{ ml}$), a saturated aqueous NaHCO_3 solution ($3 \times 20 \text{ ml}$), brine ($2 \times 20 \text{ ml}$) then dried (MgSO_4) and evaporated.

4.3.1. 2,3,5,6,8,9,11,12-Octahydronaphtho[2,3-b][1,4,7,10,13]pentaoxacyclopentadecine-16-yl acetate (**12**). From ketone **10** (0.54 g, 1.5 mmol) as viscous oil sufficiently pure for subsequent use (ca. 0.23 g, 40%), analytical sample was recrystallized from MeOH as colorless crystals, mp $133\text{--}134^\circ\text{C}$. ^1H NMR (250 MHz, CDCl_3): δ 2.33 (s, 3H, CH_3), 3.76–3.80 (m, 8H, 5'- CH_2 , 6'- CH_2 , 8'- CH_2 , 9'- CH_2), 3.94–4.00 (m, 4H, 3'- CH_2 , 11'- CH_2), 4.20–4.25 (m, 4H,

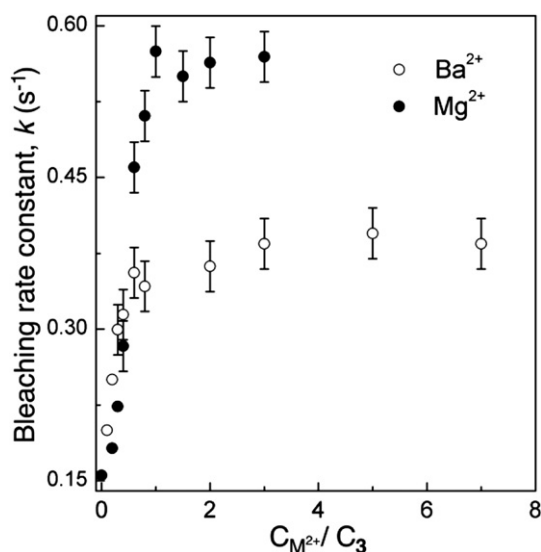


Fig. 9. Effect of metal cations on the bleaching rate constant (k) of naphthopyran **3** in acetonitrile at 299 K ($C_3=6.7 \times 10^{-3}$ M, cuvette 1 cm, $\lambda=425$ nm).

2'-CH₂, 12'-CH₂), 7.02–7.10 (m, 3H, 14'-H, 18'-H, 19'-H), 7.36 (s, 1H, 15'-H), 7.65 (d, 1H, $J=8.8$ Hz, 17'-H). ¹³C NMR (250 MHz, CDCl₃): δ 21.30, 68.40, 68.48, 69.33, 69.37, 70.33, 71.29, 107.59, 107.91, 117.33, 118.98, 127.34, 127.72, 129.73, 147.27, 149.15, 149.92, 169.93. Anal. Calcd for C₂₀H₂₄O₇·H₂O: C, 60.90; H, 6.64. Found: C, 60.96; H, 6.20.

4.3.2. 14,19-Dioxo-2,3,5,6,8,9,11,12,14,19-decahydronaphtho[2,3-*b*][1,4,7,10,13]pentaoxacyclopentadecin-16-yl acetate (**13**). From ketone **10** (0.84 g, 2.3 mmol) after eluting with 50% ethyl acetate/cyclohexane as deep yellow solid (0.03 g, 3%), mp 122–125 °C. ¹H NMR (250 MHz, CDCl₃): δ 2.34 (s, 3H, CH₃), 3.62–3.74 (m, 8H, 5'-CH₂, 6'-CH₂, 8'-CH₂, 9'-CH₂), 3.82–3.91 (m, 4H, 3'-CH₂, 11'-CH₂), 4.54–4.66 (m, 4H, 2'-CH₂, 12'-CH₂), 7.40 (dd, 1H, $J=8.4$ and 2.3 Hz, 17'-H), 7.74 (d, 1H, $J=2.3$ Hz, 15'-H), 8.07 (d, 1H, $J=8.4$ Hz, 18'-H). ¹³C NMR (250 MHz, CDCl₃): δ 21.16, 70.48, 70.52, 70.75, 70.77, 70.90, 70.96, 73.34, 73.37, 119.43, 126.84, 128.17, 128.43, 132.62, 147.22, 147.42, 155.00, 168.68, 181.19, 181.77. Anal. Calcd for C₂₀H₂₄O₁₀·H₂O: C, 56.60; H, 5.70. Found: C, 57.01; H, 5.77.

4.4. 2,3,5,6,8,9,11,12-Octahydronaphtho[2,3-*b*][1,4,7,10,13]pentaoxacyclopentadecine-16-ol (**6**)

Ester **12** (0.23 g, 0.6 mmol) was suspended in water (40 ml) and a solution of NaOH in water (30%, 20 ml) was added. The mixture was stirred at ca. 50 °C for 3 h and then cooled to room temperature. The cooled solution was extracted with dichloromethane before acidifying the aqueous layer to pH ~7 using concd HCl followed by repeated extraction with dichloromethane. The combined organic phases were washed with water to pH ~7, dried (MgSO₄), and evaporated. The residue was treated with pentane to give **6** as pale brown solid (0.12 g, 60%). An analytical sample was recrystallized from dichloromethane as colorless crystals, mp 157–158 °C. ¹H NMR (250 MHz, CDCl₃): δ 3.70–4.20 (m, 16H, crown-CH₂), 6.74 (s, 1H, 15'-H), 6.90 (dd, $J=8.7$ and 2.3 Hz, 1H, 17'-H), 6.94–7.00 (m, 2H, 14'-H, 19'-H), 7.39 (d, $J=8.7$ Hz, 1H, 18'-H). ¹³C NMR (250 MHz, CDCl₃): δ 68.01, 68.41, 69.37, 69.50, 70.32, 70.36, 71.03, 106.61, 108.41, 108.88, 115.76, 123.99, 127.89, 130.60, 147.17, 149.66, 152.87. Anal. Calcd for C₁₈H₂₂O₆: C, 64.66; H, 6.63. Found: C, 63.65; H, 6.55.

4.5. Typical procedures for chromene preparation

Procedure A. A modification of the previously reported procedure¹¹ was used. The crowned phenol (or naphthol) (1 equiv), 1,1-diphenylprop-2-yn-1-ol (1 equiv), and TsOH (0.01 equiv) were dissolved in toluene (10 ml) and stirred at ca. 70–80 °C for 3–4 h. On completion of the stirring the solvent was evaporated and the product was eluted from silica (the eluents noted below allowed $R_f=0.3$ –0.5).

Procedure B. An adaptation of the previously reported procedure^{12c} was used. A solution of titanium(IV) ethoxide (1.5 equiv) in toluene (2 ml) was added to a stirred solution of the crowned phenol (or naphthol) (1 equiv) and β -phenylcinnamaldehyde (1 equiv) in toluene (8 ml). The mixture was stirred at 100 °C for 6 h under argon atmosphere and then cooled to ca. 40 °C before adding toluene (10 ml), water (1 ml), and silica (0.5 g). The mixture was heated at 80 °C for a further 30 min. The resulting mixture was cooled to room temperature, then filtered and the precipitate formed was washed with toluene. The organic layer was separated, dried (MgSO₄), and evaporated. The product was eluted from silica.

4.5.1. 18,18-Diphenyl-2,3,5,6,8,9,11,12-octahydro-18H-[1,4,7,10,13]pentaoxacyclopentadeca[2,3-*h*]chromene (**1a**). **Procedure A:** From

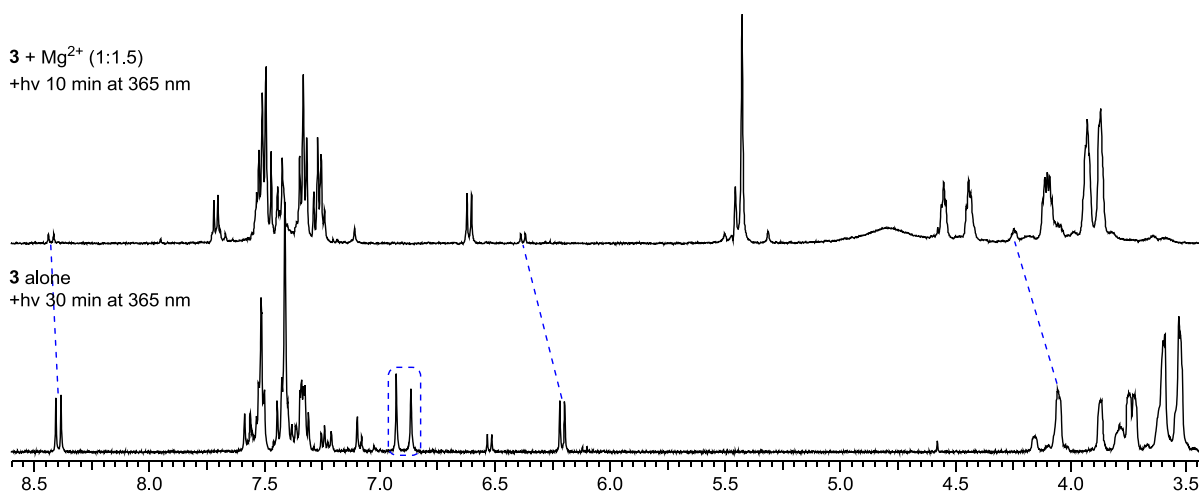


Fig. 10. ¹H NMR spectra of a solution of **3** alone and with Mg²⁺ at 1:1.5 ratio upon irradiation at 313 nm (–40 °C, CD₃CN, C₃=0.001 M).

Table 3
Crystal data and structure refinement parameters for **1a** and **6**

Compound	1a	6
CCDC	763,215	763,216
Empirical formula	C ₂₉ H ₃₀ O ₆	C ₁₉ H ₂₆ Cl ₂ O ₇
Formula weight	316.35	437.3
Crystal color, habit	Colorless prism	Colorless prism
Crystal size (mm)	0.23×0.20×0.15	0.30×0.30×0.15
Temperature (K)	100(2) K	293(2)
Crystal system	Orthorhombic	Monoclinic
Space group	<i>Pbca</i>	<i>P2₁/n</i>
<i>a</i> (Å)	9.6763(19)	9.1000(2)
<i>b</i> (Å)	17.770(4)	8.2070(2)
<i>c</i> (Å)	27.452(6)	28.9379(9)
β (°)		90.036(1)
<i>V</i> (Å ³)	4720.2(16)	2161.19(10)
<i>Z</i> (<i>Z'</i>)	8(1)	4(1)
<i>F</i> (000)	2016	920
<i>D</i> _{calcd} (g cm ⁻³)	1.335	1.334
Linear absorption, μ (cm ⁻¹)	0.93	3.37
Scan type	ω	ω
θ Range (°)	1.48–29.27	1.41–28.24
Independent reflections	6426 [<i>R</i> _{int} =0.0741]	4994 [0.071]
Observed reflections [<i>I</i> >2 σ (<i>I</i>)	4246	2468
Parameters	316	293
Final <i>R</i> (<i>F</i> _{hkl}): <i>R</i> ₁	0.0487	0.0786
<i>wR</i> ₂	0.1219	0.3226
GOF	1.015	1.16
$\Delta\rho_{\max}$, $\Delta\rho_{\min}$ (e Å ⁻³)	0.387, -0.241	0.125; -0.406

phenol **4a** (0.57 g, 2 mmol) after eluting from silica with ethyl acetate as a viscous oil (<0.01 g, <1%). See characteristics in lit.⁸

4.5.2. 21,21-Diphenyl-2,3,5,6,8,9,11,12,14,15-decahydro-21H-[1,4,7,10,13,16]hexaoxacyclooctadeca[2,3-*h*]chromene (**1b**). *Procedure A*: From phenol **4b** (0.33 g, 1 mmol) after eluting from silica with ethyl acetate as a viscous oil (<0.01 g, <1%). See characteristics in lit.⁸

4.5.3. 16,16-Diphenyl-2,3,5,6,8,9,11,12-octahydro-16H-[1,4,7,10,13]pentaaxacyclopentadeca[2,3-*g*]chromene (**2a**). *Procedure A*: From phenol **5a** (0.03 g, 0.1 mmol) after eluting from silica with 15–50% benzene/ethyl acetate as a viscous oil (0.02 g, 4%); *procedure B*: from phenol **5a** (0.57 g, 2 mmol) after eluting with 10% methanol/dichloromethane as a pale orange powder (0.19 g, 20%), mp 76–78 °C. ¹H NMR (300 MHz; CD₃CN): δ 3.58–3.70 (m, 8H, 5-CH₂, 6-CH₂, 8-CH₂, 9-CH₂), 3.72–3.83 (m, 4H, 3-CH₂, 11-CH₂), 3.96–4.02 (m, 2H, 2-CH₂), 4.04–4.12 (m, 2H, 12-CH₂), 6.25 (d, *J*=9.8 Hz, 1H, 17-H), 6.48–6.63 (m, 2H, 18-H, 14-H), 6.69 (s, 1H, 19-H), 7.22–7.65 (m, 10H, Ar-H); ¹³C NMR (75 MHz, CD₃CN): δ 68.5, 68.8, 69.2, 69.7, 69.8, 70.1, 70.4, 70.5, 82.0 (s, *quat*-C), 102.8, 112.9, 113.8, 123.3, 126.5, 126.8, 127.5, 128.2, 143.4, 145.3, 147.2, 150.4. Anal. Calcd for C₂₉H₃₀O₆: C, 73.0; H, 6.4. Found: C, 73.2; H, 6.3.

4.5.4. 19,19-Diphenyl-2,3,5,6,8,9,11,12,14,15-decahydro-19H-[1,4,7,10,13,16]hexaoxacyclooctadeca[2,3-*g*]chromene (**2b**). *Procedure A*: From phenol **5b** (0.2 g, 0.6 mmol) after eluting from silica with 10% methanol/dichloromethane as a viscous oil (0.06 g, 19%); *procedure B*: from phenol **5b** (0.33 g, 1 mmol) after eluting with 10% methanol/dichloromethane as pale orange crystals (0.13 g, 25%), mp 72–74 °C. ¹H NMR (250 MHz, CDCl₃): δ 3.58–3.72 (m, 12H, 5-CH₂, 6-CH₂, 8-CH₂, 9-CH₂, 11-CH₂, 12-CH₂), 3.77–3.88 (m, 4H, 3-CH₂, 14-CH₂), 3.96–4.08 (m, 4H, 2-CH₂, 15-CH₂), 5.94 (d, *J*=9.7 Hz, 1H, 20-H), 6.39–6.52 (m, 3H, 17-H, 21-H, 22-H), 7.11–7.29 (m, 6H, Ar-H), 7.30–7.38 (m, 4H, Ar-H). ¹³C NMR (250 MHz, CDCl₃): δ 68.56, 69.34, 69.63, 69.91, 70.53, 70.59, 70.66, 70.68, 82.43 (s, *quat*-C), 102.61, 113.23, 113.38, 123.01, 126.35, 126.87, 127.34, 127.97,

142.80, 144.83, 147.33, 150.14. Anal. Calcd for C₃₁H₃₄O₇·2H₂O: C, 67.13; H, 6.91. Found: C, 67.68; H, 6.96.

4.5.5. 3,3-Diphenyl-9,10,12,13,15,16,18,19-octahydro-3H-[1,4,7,10,13]pentaaxacyclopentadeca[2',3':4,5]benzo[1,2-*f*]chromene (**3**). *Procedure A*: From naphthol **6** (0.096 g, 0.29 mmol) after eluting from silica using 10% methanol/dichloromethane as a viscous oil (0.024 g, 16%); *procedure B*: from naphthol **6** (0.2 g, 0.6 mmol) after eluting from silica using 10% methanol/dichloromethane re-crystallization from diethyl ether as pale beige solid (0.09 g, 29%), mp 147–148 °C. ¹H NMR (250 MHz, CDCl₃): δ 3.74–3.78 (m, 8H, 12-CH₂, 13-CH₂, 15-CH₂, 16-CH₂), 3.87–3.95 (m, 4H, 10-CH₂, 18-CH₂), 4.10–4.22 (m, 4H, 9-CH₂, 19-CH₂), 6.24 (d, *J*=9.9 Hz, 1H, 2-H), 6.96 (s, 1H, 21-H), 7.04 (d, *J*=8.7 Hz, 1H, 5-H), 7.14–7.34 (m, 8H, Ar-H, 1-H, 7-H), 7.41–7.51 (m, 5H, Ar-H, 6-H). ¹³C NMR (250 MHz, CDCl₃): δ 68.46, 68.48, 69.31, 70.24, 71.09, 82.17 (s, *quat*-C), 102.56, 109.17, 113.34, 116.15, 119.69, 124.88, 125.67, 126.97, 127.43, 127.54, 128.03, 128.11, 144.90, 147.36, 149.52, 149.96. Anal. Calcd for C₃₃H₃₂O₆: C, 75.55; H, 6.15. Found: C, 75.23; H, 6.02.

4.6. X-ray crystallography

Crystals suitable for X-ray diffraction were grown by slow evaporation of solutions in CH₂Cl₂. X-ray diffraction experiments were carried out with a Bruker APEX II CCD area detector, using graphite monochromated Mo *K* α radiation (λ =0.71073 Å, ω -scans). Reflection intensities were integrated using SAINT software and absorption correction was applied semi-empirically using SADABS program. The structures were solved by direct method and refined by the full-matrix least-squares against *F*² in anisotropic approximation for non-hydrogen atoms. Hydrogen atoms of the water molecule were located from the Fourier density synthesis. In the crystal of **6**, the solvate CH₂Cl₂ molecule is disordered over three positions with occupancies equal to 0.75, 0.15, and 0.15. Crystal data and structure refinement parameters for **1a** and **6** are given in Table 3. All calculations were performed using the SHELXTL software.

4.7. Spectrokinetic measurements

UV absorption spectra were recorded using an Agilent HP-8453 spectrophotometer (Agilent Technologies) with the characteristic time of recording ca. 2 s. High pressure mercury lamp with the set of glass filters was used as a light source for stationary photolysis. To measure rate constants of the dark reactions with the characteristic time of several seconds, samples were irradiated in the cuvette box of the spectrophotometer. The irradiation was performed till the equilibrium between closed and open forms (photostationary state) was achieved. The achievement of photostationary conditions was controlled by the absorption of the open form in the visible spectral region. After that the irradiation was interrupted and the kinetic curves corresponding to the recovery of the system to the initial closed state were recorded.

NMR spectra were recorded on a Bruker 500 spectrometer (1H, 500 MHz) equipped with TXI probe, using standard sequences. Photoirradiation was carried out directly into the NMR tube in a home-built apparatus with a 1000 W high-pressure Hg–Xe lamp equipped with a filter (Schott 11FG09: 259< λ <388 nm with λ_{\max} =330 nm, *T*=79%) to select UV light and an interferential filter (λ =313 nm).

Acknowledgements

Financial support from Réseau Formation-Recherche Franco-Russe du Ministère de l'Enseignement Supérieur et de la Recherche (MENESR), the Russian Foundation for Basic Research, Program of Russian Academy of Sciences, and ARCUS program are greatly

appreciated. The NMR facilities were funded by the Region Nord-Pas de Calais (France), the Ministère de la Jeunesse de l'Éducation Nationale et de la Recherche (MJENR), and the Fonds Europeens de Developpement Regional (FEDER). Part of this collaborative work was realized within the framework GDR CNRS 93 'Phenics' (Photoswitchable Organic Molecular Systems & Devices).

Supplementary data

Supplementary data related to this article can be found online at <http://dx.doi.org/10.1016/j.tet.2012.07.029>.

References and notes

- (a) *Organic Photochromic and Thermochromic Compounds*; Crano, J. C., Guglielmetti, R. J., Eds.; Kluwer Academic/Plenum: New York, NY, 1999; Vol. 1; (b) *Photochromism: Molecules and Systems*; Durr, H., Bouas-Laurent, H., Eds.; Elsevier: Amsterdam, 1990; (c) *Photochromism*; Brown, G. H., Ed.; Wiley Interscience: New York, NY, 1971.
- (a) Tsigvoulis, G.; Lehn, J.-M. *Angew. Chem., Int. Ed. Engl.* **1995**, *34*, 1119–1122; (b) Berkovic, G.; Krongauz, V.; Weiss, V. *Chem. Rev.* **2000**, *100*, 1741–1754; (c) Irie, M. *Chem. Rev.* **2000**, *100*, 1685–1716.
- Descalzo, A. B.; Martínez-Mañez, R.; Sancenón, F.; Hoffmann, K.; Rurack, K. *Angew. Chem., Int. Ed.* **2006**, *45*, 5924–5948.
- (a) Ahmed, S. A.; Tanaka, M.; Ando, H.; Iwamoto, H.; Kimura, K. *Tetrahedron* **2003**, *59*, 4135–4142; (b) Paramonov, S.; Lokshin, V.; Fedorova, O. *J. Photochem. Photobiol., C* **2011**, *12*, 209–236.
- (a) Liondagan, M.; Willner, I. *J. Photochem. Photobiol., A* **1997**, *108*, 247–252; (b) Willner, I.; Rubin, S.; Shatzmiller, R.; Zor, T. *J. Am. Chem. Soc.* **1993**, *115*, 8690–8694; (c) Willner, I.; Rubin, S. *Angew. Chem., Int. Ed.* **1996**, *35*, 367–385; (d) Takase, M.; Inouye, M. *Chem. Commun.* **2001**, 2432–2433; (e) Paramonov, S.; Lokshin, V.; Ihmels, H.; Fedorova, O. *Photochem. Photobiol. Sci.* **2011**, *10*, 1279–1282.
- (a) Tanaka, M.; Kamada, K.; Ando, H.; Kitagaki, T.; Shibuyani, Y.; Kimura, K. *J. Org. Chem.* **2000**, *65*, 4342–4347; (b) Nakamura, M.; Fujioka, T.; Sakamoto, H.; Kimura, K. *New J. Chem.* **2002**, *26*, 554–559; (c) Fedorova, O. A.; Gromov, S. P.; Alifimov, M. V. *Russ. Chem. Bull.* **2001**, *50*, 1970–1983; (d) Kimura, K.; Sakamoto, H.; Nakamura, M. *Bull. Chem. Soc. Jpn.* **2003**, *76*, 225–245; (e) Alifimov, M. A.; Fedorova, O. A.; Gromov, S. P. *J. Photochem. Photobiol., A* **2003**, *158*, 183–198.
- (a) Ahmed, S. A.; Tanaka, M.; Ando, H.; Iwamoto, H.; Kimura, K. *Tetrahedron* **2004**, *60*, 3211–3220; (b) Glebov, E.; Smolentsev, A.; Korolev, V.; Plyusnin, V.; Chebun'kova, A.; Paramonov, S.; Fedorova, O.; Lokshin, V.; Samat, A. *J. Phys. Org. Chem.* **2009**, *22*, 537–545; (c) Fedorova, O. A.; Strokach, Y. P.; Chebun'kova, A. V.; Valova, T. M.; Gromov, S. P.; Alifimov, M. V.; Lokshin, V.; Samat, A. *Russ. Chem. Bull.* **2006**, *55*, 287–294; (d) Ushakov, E. N.; Nazarov, V. B.; Fedorova, O. A.; Gromov, S. P.; Chebun'kova, A. V.; Alifimov, M. V.; Barigelletti, F. *J. Phys. Org. Chem.* **2003**, *16*, 306–309; (e) Fedorova, O. A.; Maurel, F.; Ushakov, E. N.; Nazarov, V. B.; Gromov, S. P.; Chebun'kova, A. V.; Feofanov, A. V.; Alaverdian, I. S.; Alifimov, M. V.; Barigelletti, F. *New J. Chem.* **2003**, *27*, 1720–1730; (f) Kumar, A.; Van Gemert, B.; Knowles, D. B. *Mol. Cryst. Liq. Cryst.* **2000**, *334*, 217–222.
- Paramonov, S. V.; Fedorova, O. A.; Perevalov, V. P.; Lokshin, V.; Khodorkovsky, V. *Russ. Chem. Bull.* **2008**, *57*, 2381–2384.
- Wada, F.; Arata, R.; Goto, T.; Kikukawa, K.; Matsuda, T. *Bull. Chem. Soc. Jpn.* **1980**, *53*, 2061–2963.
- (a) Godfrey, I. M.; Sargent, M. V.; Elix, J. A. *J. Chem. Soc., Perkin Trans. 1* **1974**, 1353–1354; (b) Smyth, M. S.; Stefanova, I.; Horak, I. D.; Burke, T. R. *J. Med. Chem.* **1993**, *36*, 3015–3020.
- Iwai, I.; Ide, J. *Chem. Pharm. Bull.* **1963**, *11*, 1042–1049.
- (a) Pozzo, J. L.; Lokshin, V. A.; Guglielmetti, R. *Mol. Cryst. Liq. Cryst.* **1994**, *246*, 75–78; (b) Pozzo, J. L. Ph.D. Thesis, Université de la Méditerranée, Marseille, France, 1994; (c) Malatesta, V.; Hobbey, J.; Giroladini, W.; Wis, M. L. U.S. Patent 0006589A1, 2002.
- Camps, F.; Coll, J.; Ricart, S. *J. Heterocycl. Chem.* **1983**, *20*, 249–250.
- Arnaud-Neu, F.; Delgado, R.; Chaves, S. *Pure Appl. Chem.* **2003**, *75*, 71–102.
- (a) Beck, M.; Nagypal, I. *Chemistry of Complex Equilibria*; Academiai Kiado: Budapest, 1989; (b) Connors, K. A. *Binding Constants: the Measurement of Molecular Complex Stability*; Wiley, John, Incorporated: New York, NY, 1987.
- Hargrove, A.; Zhong, Z.; Sessler, J.; Anslyn, E. *New J. Chem.* **2010**, *34*, 348–354.
- Gromov, S.; Vedernikov, A.; Ushakov, E.; Kuz'mina, L.; Feofanov, A.; Avakyan, V.; Churakov, A.; Alaverdyan, Y.; Malysheva, E.; Alifimov, M.; Howard, J.; Eliasson, B.; Edlund, U. *Helv. Chim. Acta* **2002**, *85*, 60–81.
- Paramonov, S.; Delbaere, S.; Fedorova, O.; Fedorov, Y.; Lokshin, V.; Samat, A.; Vermeersch, G. *J. Photochem. Photobiol., A* **2010**, *209*, 111–120.
- (a) Ushakov, E.; Gromov, S.; Fedorova, O.; Pershina, Y.; Alifimov, M.; Barigelletti, F.; Flamigni, L.; Balzani, V. *J. Phys. Chem. A* **1999**, *103*, 11188–11193; (b) Fedorov, Y.; Fedorova, O.; Andryukhina, E.; Gromov, S.; Alifimov, M.; Kuzmina, L.; Churakov, A.; Howard, J.; Aaron, J.-J. *New J. Chem.* **2003**, *27*, 280–288.
- Davis, J.; Foster, T.; Tonelli, M.; Butcher, S. *RNA* **2007**, *13*, 76–86.
- Hepworth, J. D.; Heron, B. M. In *Functional Dyes: Photochromic Naphthopyrans*; Kim, S.-H., Ed.; Elsevier: Amsterdam, 2006; pp 85–135.
- Simonet, J.; Patillon, H.; Belloncle, C.; Simonet-Gueguen, N.; Cauliez, P. *Synth. Met.* **1995**, *75*, 103–110.
- Parish, W. W.; Scott, P. E.; McCausland, C. W.; Bradshaw, J. S. *J. Org. Chem.* **1978**, *43*, 4577–4581.